Available on CMS information server

CMS DN-2007/009

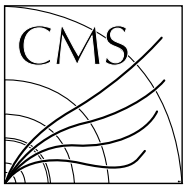

The Compact Muon Solenoid Experiment

Detector Note

The content of this note is intended for CMS internal use and distribution only

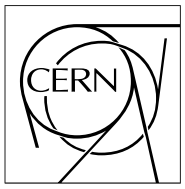

15 May 2007 (v3, 19 September 2008)

Pre-calibration of the CMS ECAL with cosmic ray muons

T. Camporesi, F. Cavallari, G. Della Ricca, F. Ferri, G. Franzoni,A. Ghezzi, B. Gobbo, D. Gong, J. Haupt, P. Musella, A. Palma, S. Ragazzi, P. Rumerio, R. Rusack, T. Tabarelli de Fatis, E. Vlasov

Abstract

This rapid note describes the pre-calibration of the ECAL barrel with muons from cosmic ray. The set up for the data taking and the pre-calibration techniques are briefly described and the results of the inter-calibration are reported.

1 Introduction

The Compact Muon Solenoid (CMS) experiment [1] is a general purpose detector which will operate at the LHC proton-proton collider at CERN. The experiment is equipped with a hermetic homogeneous electromagnetic calorimeter (ECAL) [2] made of lead tungstate ($PbWO_4$) crystals. The crystal material has been chosen for its fast response and its resistance to irradiation as well as its high density (8.3 g/cm^3), short radiation length ($X_0 \simeq 0.89$ cm) and small Moliere radius ($R_M \simeq 2.19$ cm), allowing a compact detector to be built. ECAL has been designed to provide the granularity and the excellent energy resolution which are required to detect the decay of the Standard Model Higgs boson into two photons.

The barrel of ECAL is divided into two halves, each composed of 18 supermodules containing 1700 crystals. There are 4 modules in each supermodule separated by aluminum webs. The individual crystals have a truncated-pyramid shape with a lateral size of approximately 1 R_M and a length of $25.8X_0$. After the assembly the response of the different channels has a spread of about 13%, therefore the calibration of the detector is mandatory.
An ultimate inter-calibration at the 0.5 % level is expected to be achieved *is situ* employing physics events. Still an initial inter-calibration at the percent level is required to guarantee an acceptable performance at the startup. To this end, all the ECAL barrel supermodules are exposed to cosmic ray muons before their installation in CMS.
In the inter-calibration with muons from cosmic rays, the calibration signal is provided by the energy released by the muons, interacting as minimum ionizing particles crossing the ECAL crystals, with about 250 MeV of deposited energy. This energy is well above the electronic noise.

2 Principles of the inter-calibration with cosmic ray μ

The experimental setup for the data taking with cosmic rays is shown in figure 1. It hosts one super-modules at a time. The data acquisition is triggered by the coincidence of a layer of plastic scintillators placed immediately under the bottom face of the super-module and of a plastic scintillator placed in the focal point. This geometry helps to select muons directed along the crystal axis. To increase the rate of aligned muons at large η, in the fourth module, the super-module is inclined by 10 degrees with respect to the horizontal position.

The data analysis exploits two different techniques on independent data samples. Events with sizable energy deposit either in one single crystal or in two nearby crystals are selected. A signal of at least 10 ADC counts is required in the "single crystal" sample and of at least 3 ADC counts in each crystal and 12 ADC counts in total in the "crystal pair" sample. As schematically shown in figure 2), crystal pairs can be aligned along iη or along iϕ (respectively "pairs at constant iη" and "pairs at constant iϕ" in the following)[1)]. In all the samples the surrounding crystals are used as a veto by requiring a signal below 3 ADC counts in each of them, approximately 3 σ above the electronic noise level.

In order to achieve a reasonable veto efficiency, during the data taking with cosmic rays the APD readout photodetectors are operated at a gain increased by a factor four with respect to the nominal gain of 50 used during standard operation in CMS and during the test beam. The increase of the APD gain also improve the signal over noise ratio. A precise measurement of the ratio between the two gains is obtained by looking at the readout response to the injection of a laser light.

The inter-calibrations are obtained equalizing the responses of the different crystals to the muons.

Coefficients issued from the cosmic ray calibration are compared to inter-calibration coefficients provided by electron test beam data [3], used as reference. This allows to determine for each of the cosmic ray inter-calibration methods the overall precision and its dependence along iη. With such information, the three set of inter-calibration coefficients from cosmic ray muons are combined with a weighted mean in a single one and a final precision ranging from 1.3% to 2% depending on iη is achieved.

2.1 Some remarks

All the comparisons with the calibration with electrons have been performed employing the test beam calibrations with the S1 technique [3].

[1)] In this note the indexes iη and iϕ identify the crystal position within a supermodule. With reference to the CMS standard coordinate system they scan the pseudo-rapidity and the azimuthal angle respectively.

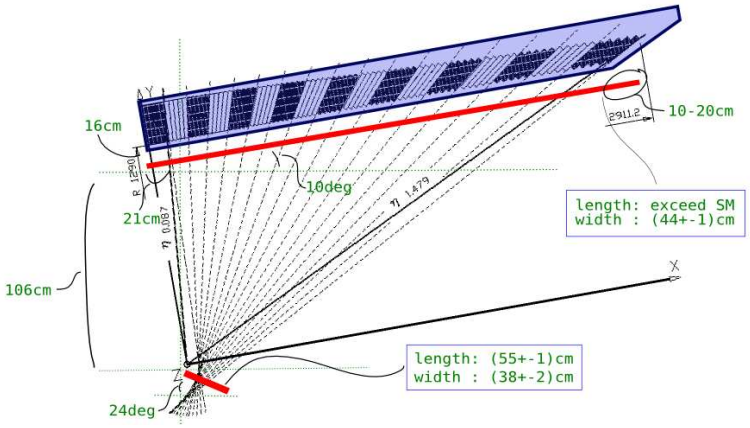

Figure 1: Experimental setup for the data taking with cosmic muons. The thick red lines placed below the super-module and close to the interaction point represent the trigger scintillator.

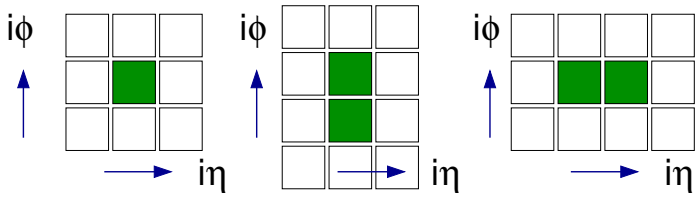

Figure 2: Schematic view of the topology of the selected events in the different samples ("single","pairs at constant iη" and "pairs at constant iϕ", from left to right). The energy is deposited in the crystals colored in green, while the white crystals are used as veto, requiring that less than 3 ADC counts are registered in each vetoed crystal.

All the results from the calibration with cosmic rays here reported, unless differently explicitly stated, concern the "absolute" inter-calibration, meaning with the term "absolute" the inter-calibration that takes into account not only the inter-calibration of the crystals in a single super-module but also the inter-calibration between different super-modules.

3 Results

Figure 3 shows the number of selected events in the different samples for 10 days of data taking. The percentages of selected events in the different samples, with respects to the triggered events are 10.5%, 6.5% and 9.2% respectively for the "single crystal", "pairs at constant iη" and "pairs at constant iϕ' samples.

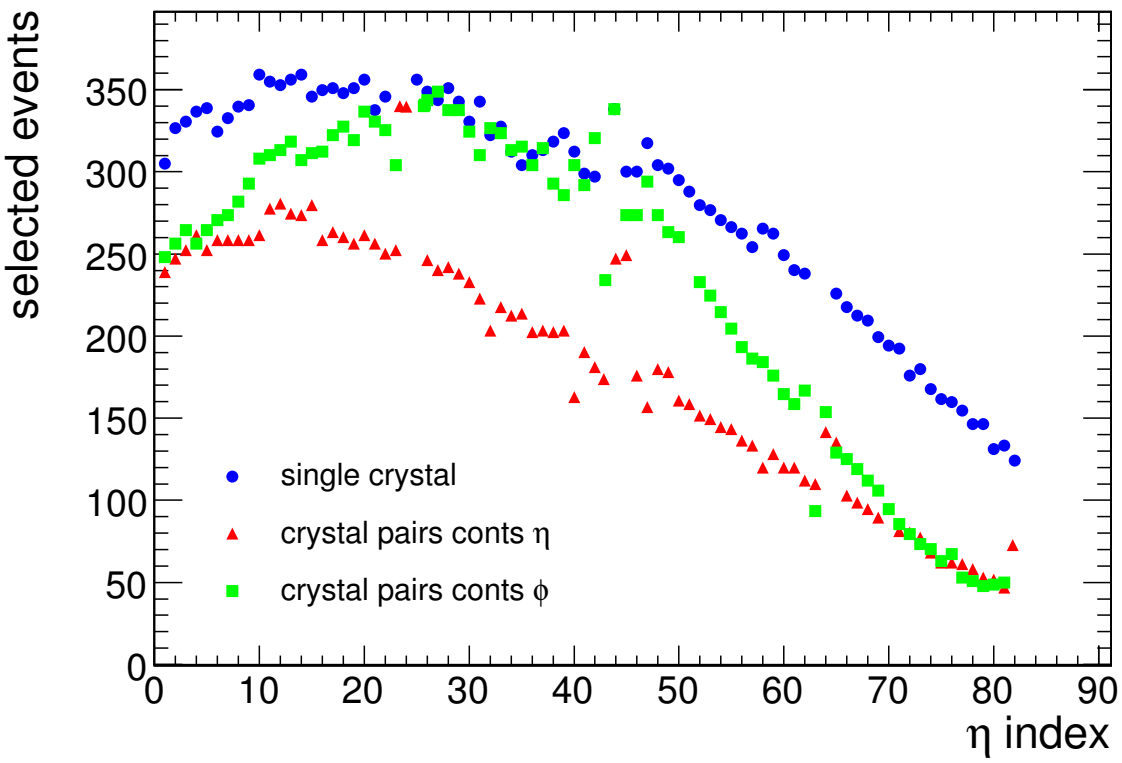

Figure 3: Number of selected events in the different samples, versus the η index. The numbers refers to 10 days of data taking.

The typical energy distribution (in ADC counts) after the selections for the single crystal analysis is plotted in figure 4, in blue (red) for a crystal in module 1 (module 4). The distribution is obtained by merging the data from different crystals scaled for the proper calibration coefficients obtained at the test beam.
Being the APDs operated at gain 200, the scale to convert the ADC counts into deposited energy is roughly 9.25 (37/4) MeV per ADC channel.

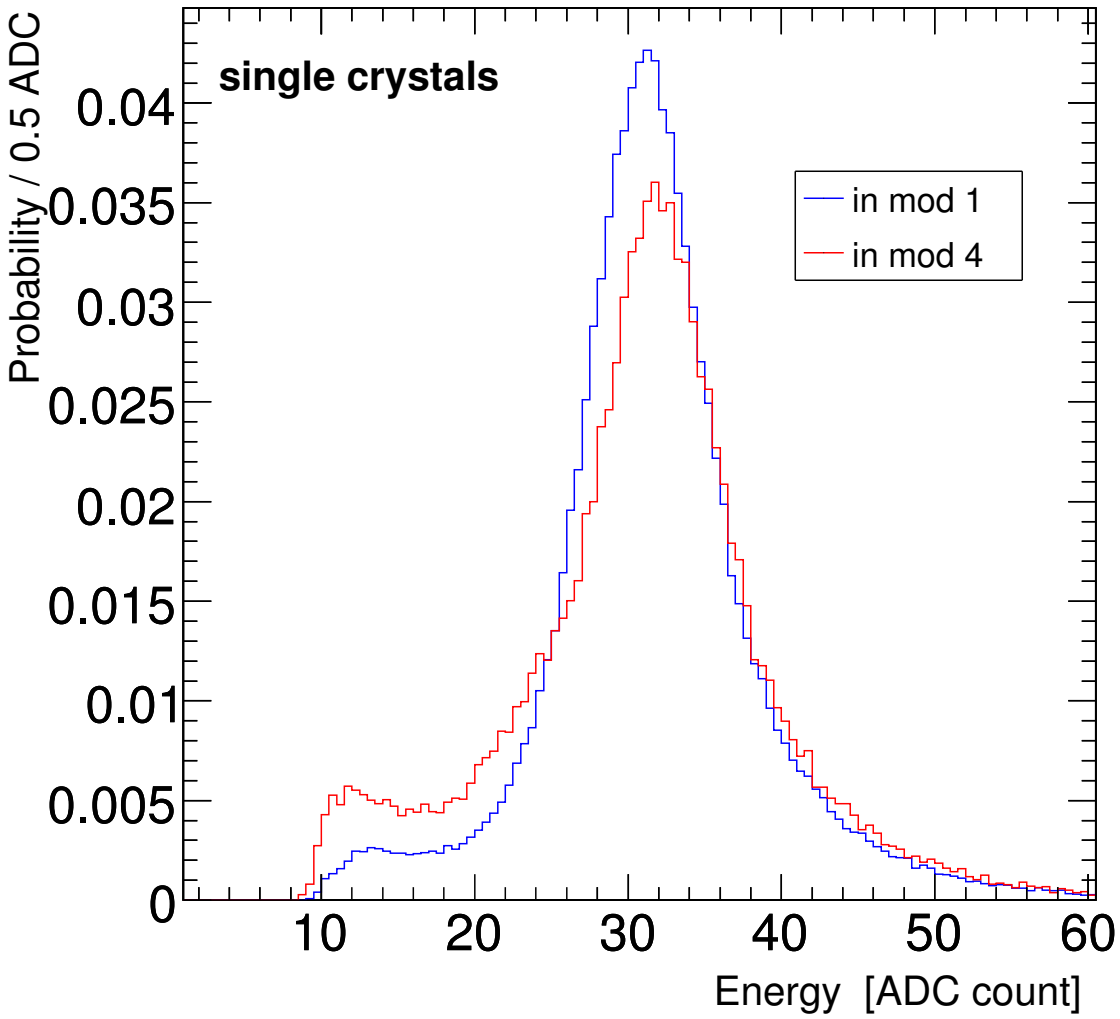

Figure 4: Distribution of the measured energy in single crystals after the selections of the "single crystal" sample, for a typical crystal in module 1 in blue and in module 4 in red.

The typical energy distribution (in ADC counts) after the selections for the crystal pairs analysis (same iη and same iϕ) is plotted in figure 5. Theses distributions are obtained by merging the data from different crystals scaled for the proper calibration coefficients for specific values of iη.
Being the APDs operated at gain 200, the scale to convert the ADC counts into deposited energy is roughly 37/4 MeV per ADC channel.

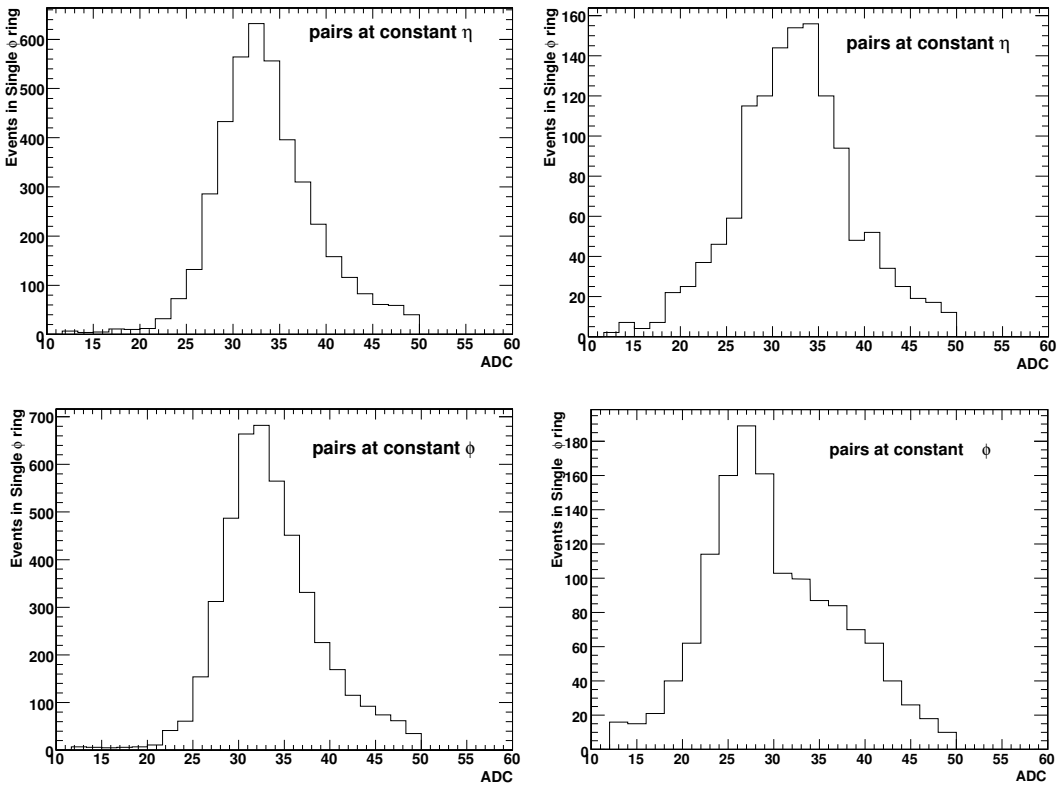

Figure 5: Distribution of the measured energy in crystal pairs after the selections of the "crystal pair" samples, for a typical pair at constant iη in module 1, top left and module 4 top right. The plots on the bottom represent the distributions for a pair at constant iϕ, in module 1 (left) and in module 4 (right).

Comparison of the inter-calibration from the **single crystal analysis** and the reference inter-calibration from the test beam, for the super-modules calibrated at the test beam (6, 12, 16, 17, 18, 22, 25). The difference $1-C_{cosm}/C_{beam}$ for all the crystal in the different super-modules is plotted in figure 6.
The crystals at the boundary of the super-module are not included in this plot, the ones placed at the boundary between modules are included.

The overall (over the whole η range, merging all the super-modules) precision is 1.7%, measured as the σ from a Gaussian fit in the peak region.

The overall (over the whole η range) precision for the crystals placed at the super-module boundaries is 3.1% (the corresponding plot is not reported).

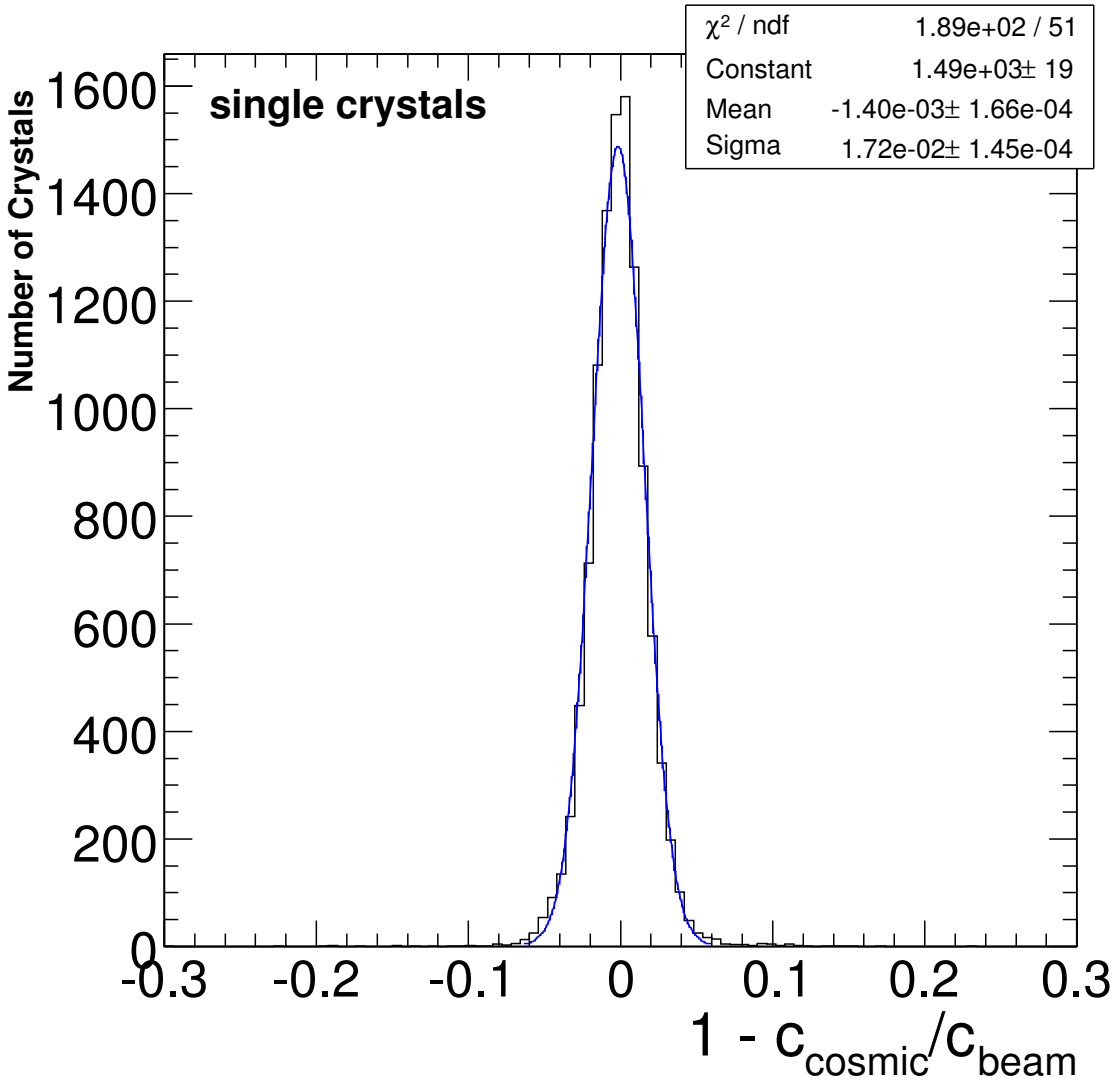

Figure 6: Distribution of the fractional difference between the calibration coefficients measured at the test beam and the ones measured with cosmic rays, with the "single crystal" technique. A Gaussian fit to the distribution is super-imposed.

Comparison of the inter-calibration from the **crystal pair analysis** and the reference inter-calibration from the test beam, for the super-modules calibrated at the test beam (6, 12, 16, 17, 18, 22, 25). The difference $1-C_{cosm}/C_{beam}$ for all the crystals in the different super-modules is plotted in figure 7, separately for the pairs at constant iη and constant iϕ.
The crystals at the boundaries of the super-module are not included in this plot, the ones placed at the boundary between modules are included.

The overall (over the whole η range, merging all the super-modules) precision is 3.4% and 3.2%, respectively for the constant iη and constant iϕ pairs, measured as the σ from a Gaussian fit in the peak region.

The overall (over the whole η range) precision for the crystals placed at the super-module boundaries is 4.4% and 3.3%, respectively for the constant iη and constant iϕ pairs (the corresponding plots are not reported).

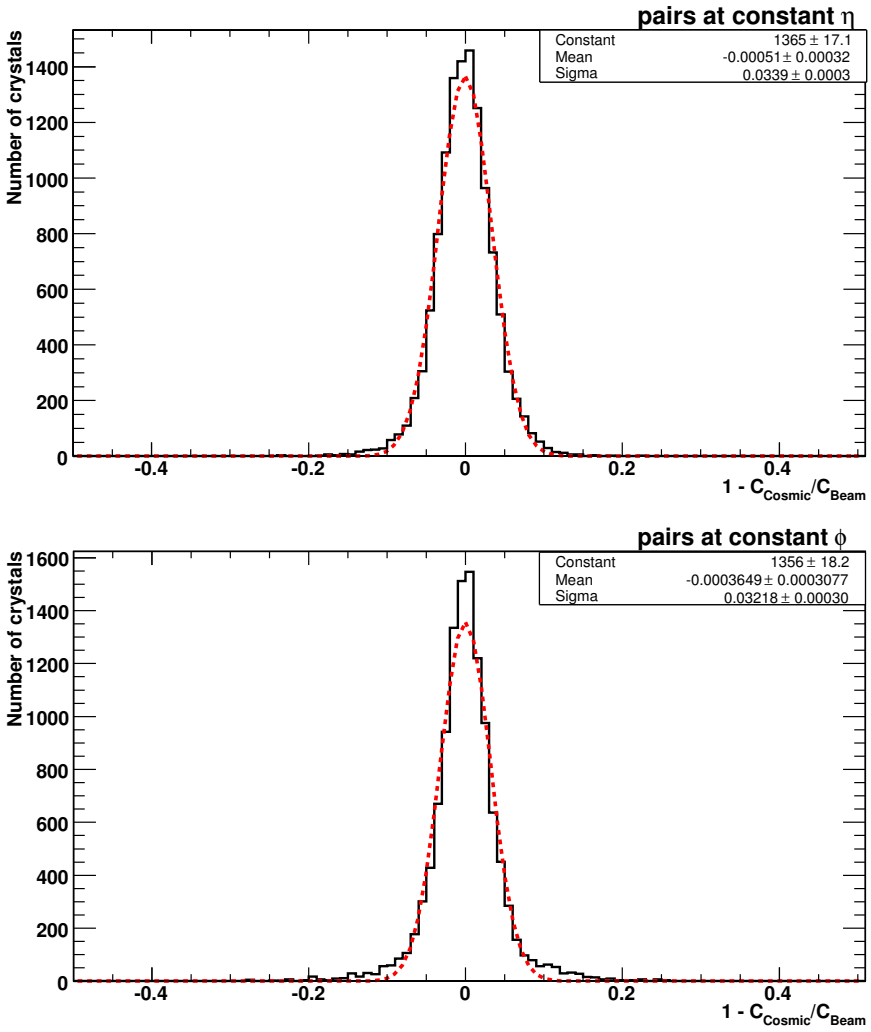

Figure 7: Distribution of the fractional difference between the calibration coefficients measured at the test beam and the ones measured with cosmic rays, from the crystal pairs at constant iη (top) and at constant iϕ (bottom). A Gaussian fit to the distribution is super-imposed.

Comparison of the inter-calibration from the **crystal pairs analysis** and the reference inter-calibration from the test beam, for the super-modules calibrated at the test beam (6, 12, 16, 17, 18, 22, 25). The coefficients from the cosmic ray calibration are obtained combining the results from the pairs at constant iη and the ones from the pairs at constant iϕ. The difference $1 - C_{cosm}/C_{beam}$ for all the crystals in the different super-modules is plotted in figure 8.
The crystals at the boundary of the super-module are not included in this plot, the ones placed at the boundary between modules are included.

The overall (over the whole η range, merging all the super-modules) precision is 2.5%, measured as the σ from a gaussian fit in the peak region.

The overall (over the whole η range) precision for the crystals placed at the super-module boundaries is 2.9% (the corresponding plot is not reported).

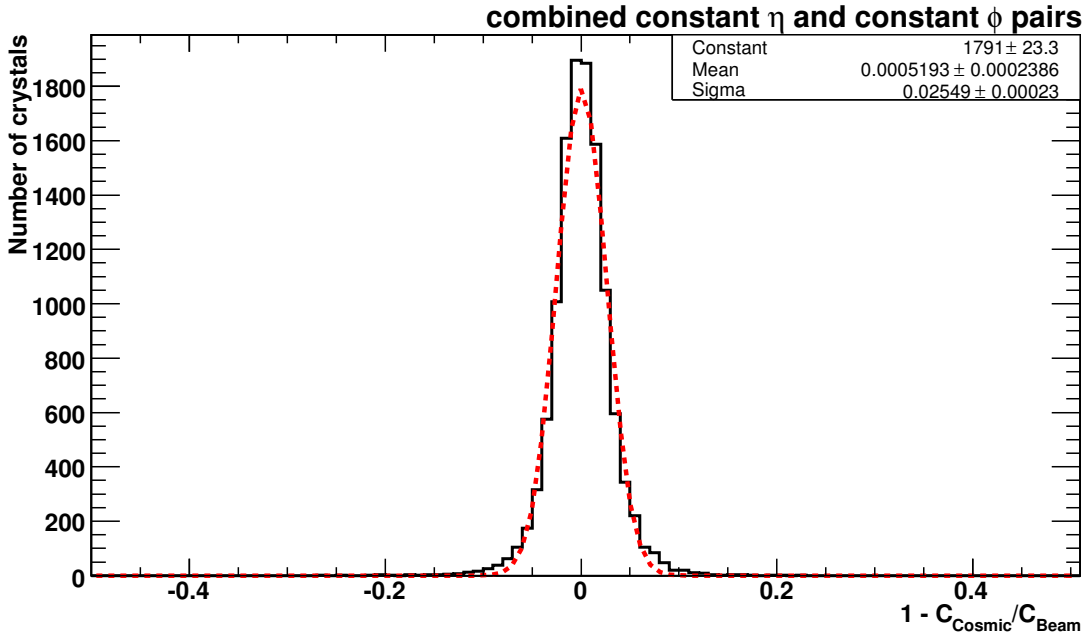

Figure 8: Distribution of the fractional difference between the calibration coefficients measured at the test beam and the ones measured combining, the results from pairs at constant iη and pairs at constant iϕ. A Gaussian fit to the distribution is super-imposed.

The plots presented in figure 9 show the statistical precision on the calibration coefficients from the different analysis, as a function of iη, for an accumulated number of 5 millions triggered events per super-module. This is obtained comparing the results from two separate sub-sample of the data, each with half the statistic of the whole sample.
The difference in the accuracy at large η between the crystal pairs at constant η and crystal pairs at constant ϕ is mainly due to the difference in the RMS of the corresponding energy distributions.

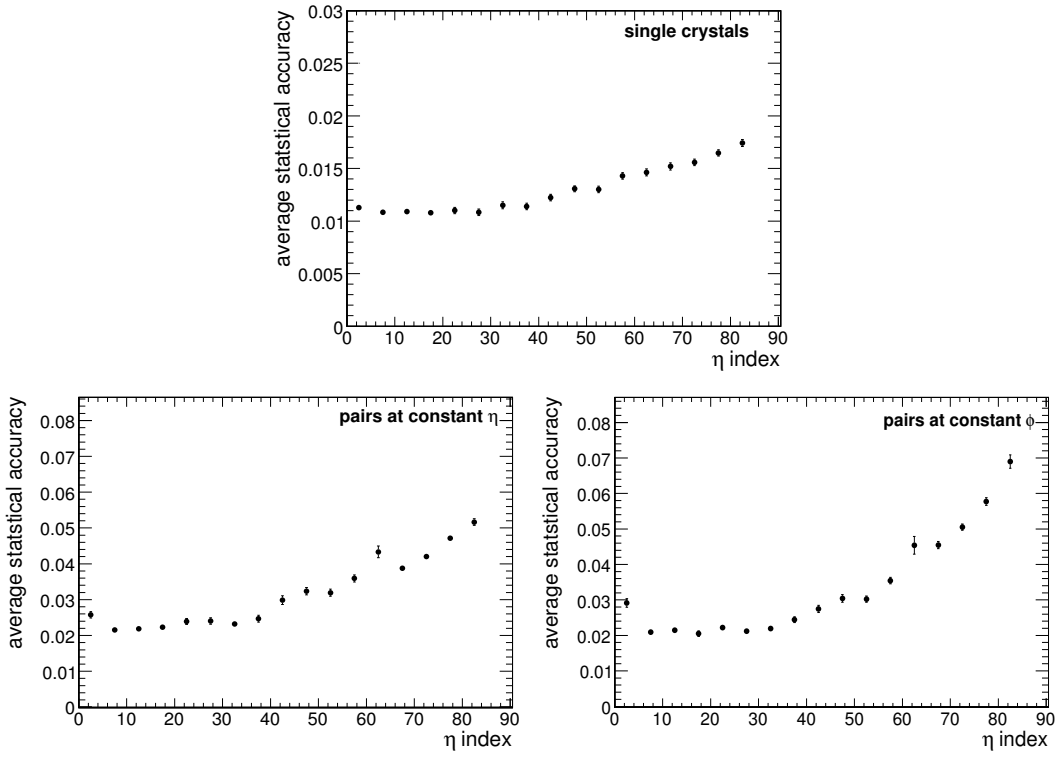

Figure 9: Statistical precision of the calibration coefficients from the different analysis: singles crystal (left), crystal pairs at constant iη (middle) and crystal pairs at constant iϕ (right).

Figure 10 show the calibration coefficients obtained by combining the results of the single crystal and crystal pairs, plotted versus the coefficients obtained at the test beam, in different colors for the different super-modules.

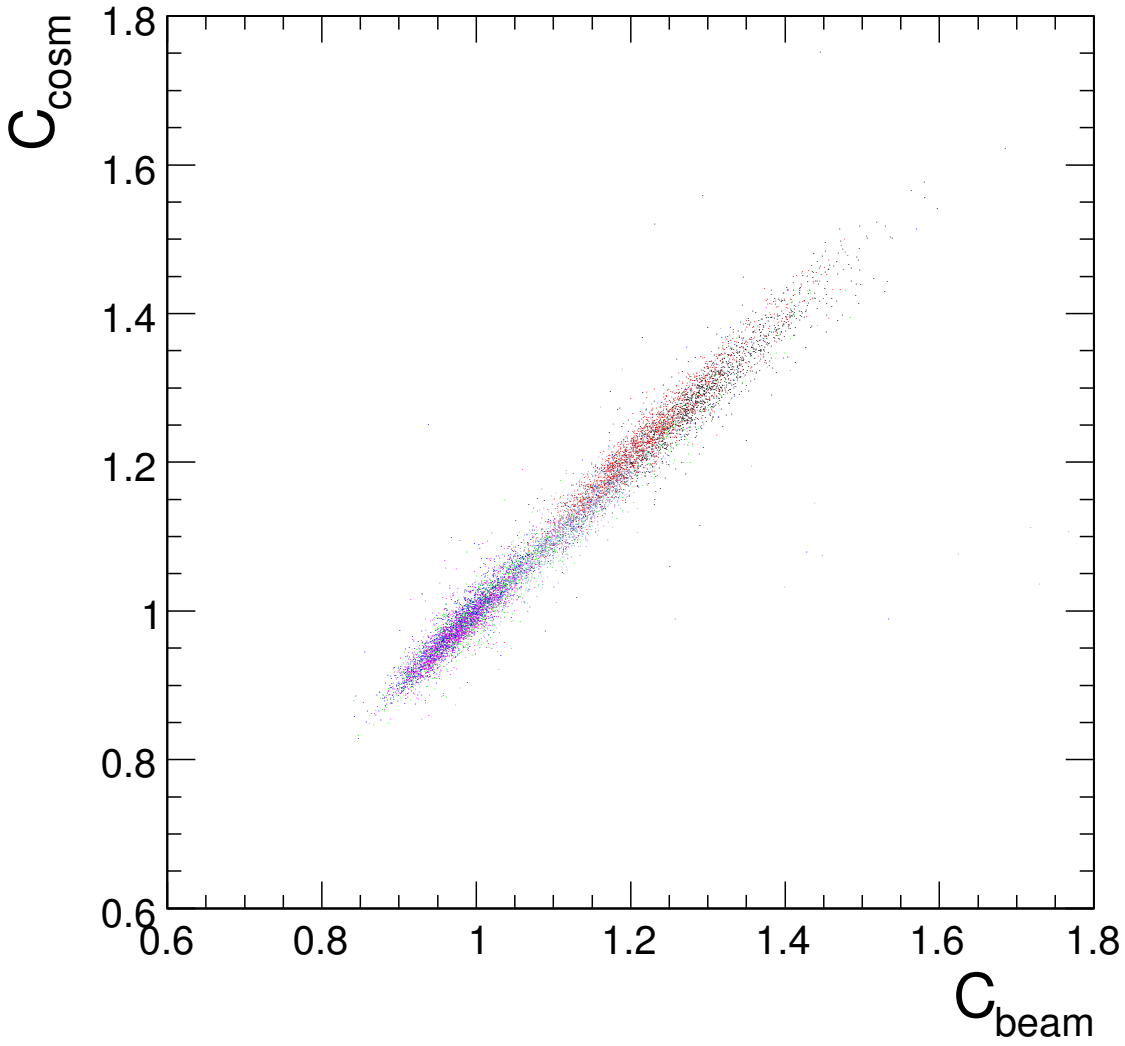

Figure 10: Calibration coefficients from the test beam vs coefficients from the cosmic rays (single crystal and crystal pairs combined). The different super-modules are plotted with different colors.

Figure 11 show the distribution of the differences in the calibration coefficients obtained by combining the results of the single crystal and crystal pairs, and the ones obtained at the test beam ($1 - C_{cosm}/C_{beam}$).

The crystals at the boundary of the super-module (edge crystals) and the ones placed at the boundary between modules are included in the plot.

The overall (over the whole η range) precision is 1.5%, measured as the σ from a gaussian fit in the peak region.

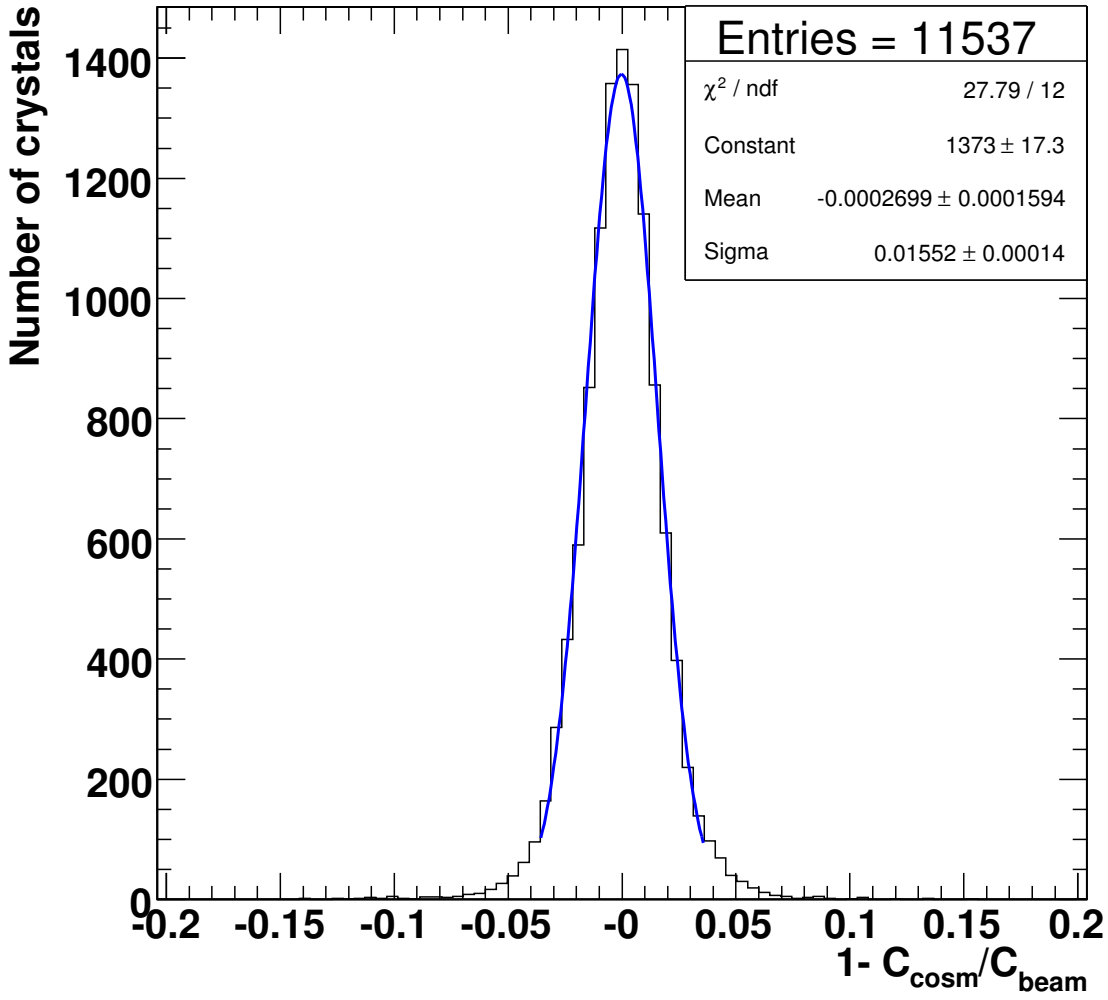

Figure 11: Distribution of the fractional difference between the calibration coefficients measured at the test beam and the ones measured combining, the results from the three different samples (single, constant iη and constant iϕ) of the cosmic ray calibration. A Gaussian fit to the distribution in the region around the peak is super-imposed.

The overall (over the whole η range) precision for the crystals placed at the super-module boundaries is 2.5% (the corresponding plot is not reported).
Excluding the edge crystals, the precision is 1.3% in module1, 1.4% in module 2, 1.4% in module 3 and 1.9% in module 4.

In figure 12 the average difference in the calibration coefficients from the test beam and from the cosmic rays $(1 - C_{cosm}/C_{beam})$ is plotted versus iη in different colors for the different super-modules. Each point in the plot is the average of the distribution of the differences, taken on slices of 5 crystals along iη (and 18 crystals along iϕ with the border excluded).

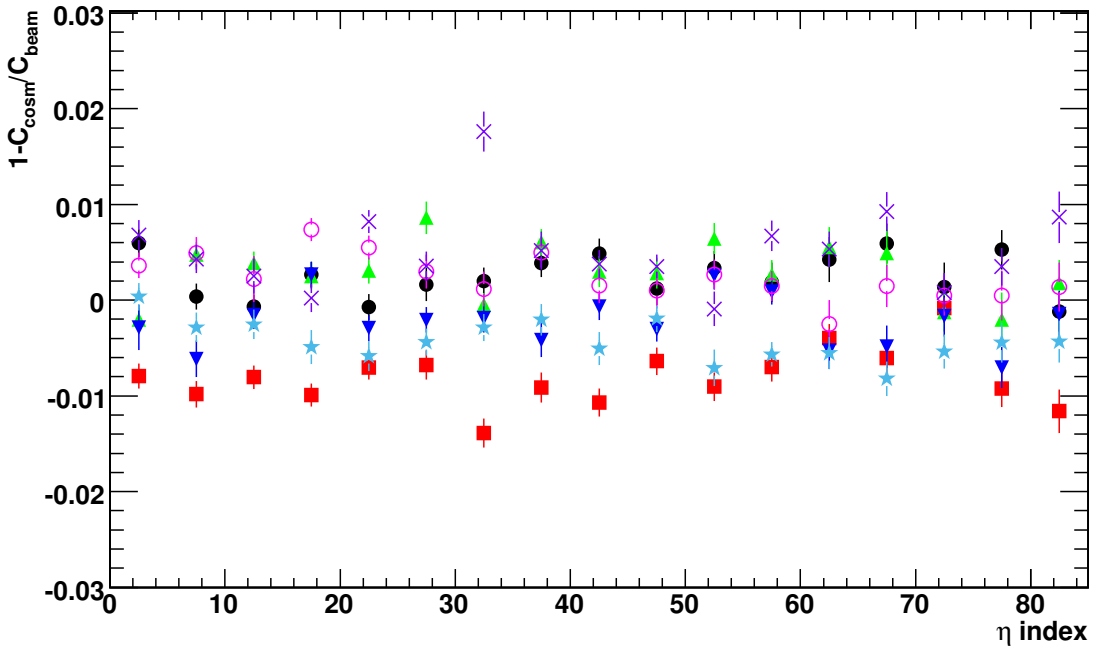

Figure 12: Average difference in the calibration coefficients from the electron beam and from the cosmic muons, plotted versus iη, in different colors for the different super-modules

Figure 13 shows the accuracy of the calibration with cosmic muons for different η regions. The accuracy is defined as the σ of the gaussian fit to the distribution of the difference in the calibrations obtained with the electrons beam and the cosmic muons ($1-C_{cosm}/C_{beam}$ as in the previous plots). For a given iη range the distribution is obtained merging the crystals from the different super-modules calibrated at the test beam (6, 12, 16, 17, 18, 22, 25). The first η slice contains 15 crystals along iη, all the other slices contain 10 crystals along iη.

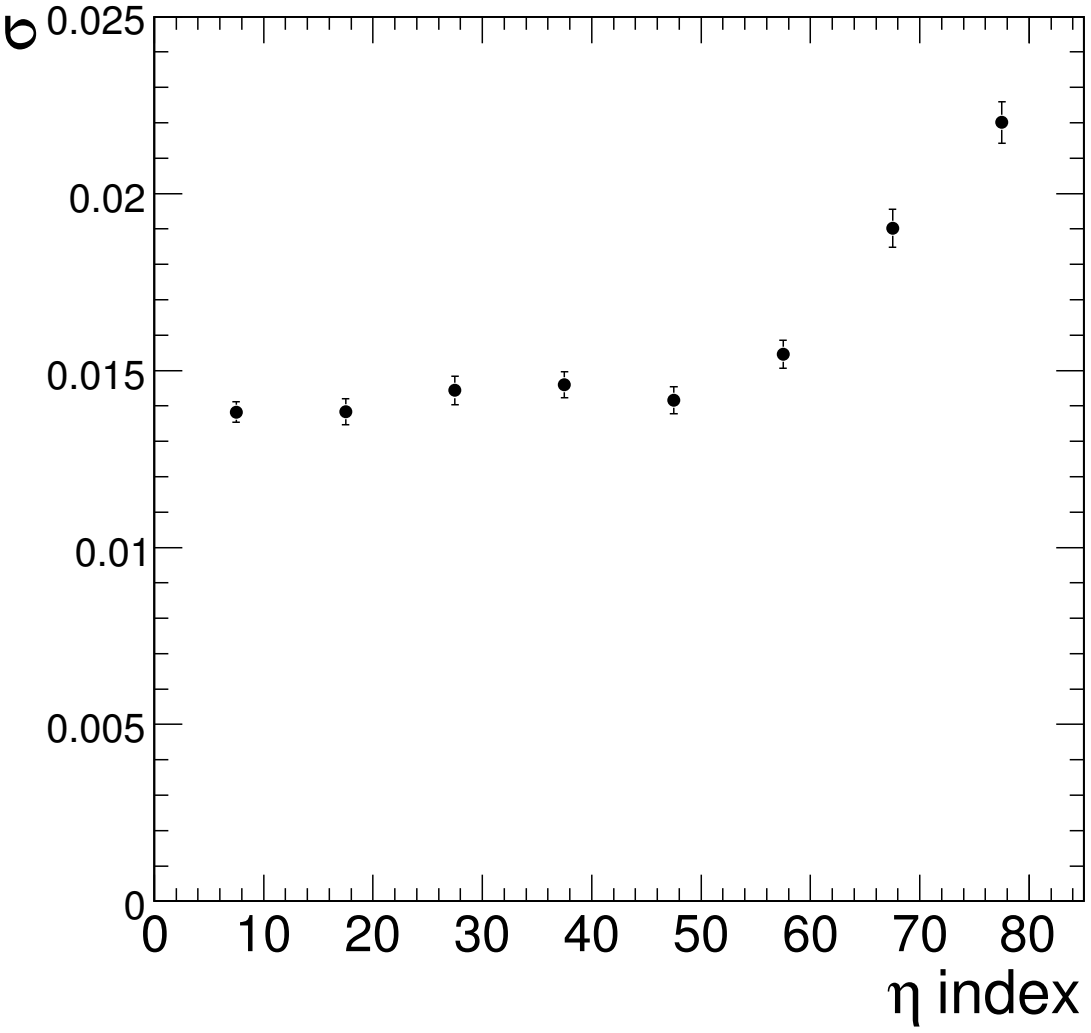

Figure 13: Accuracy of the calibration from cosmic muons vs iη

References

[1] CMS Collaboration, "The Compact Muon Solenoid - Technical Proposal", CERN/LHCC 94-38

[2] CERN/LHCC 97-33, CMS collaboration, "The electromagnetic calorimeter project. Technical Design Report.".

[3] CMS DN-2007/001, A. Benaglia *et al.* "Intercalibration at 2006 ECAL testbeam with the single crystal technique".